J Mater Sci (2024) 59:14078–14093

Polymers & biopolymers

Accelerated multistep thermal stabilization of polyacrylonitrile fibers using an ethylenediamine pretreatment

Kemal Şahin Tunçel[1,*], Tuba Demirel[2], and Ismail Karacan[3]

[1] Department of Traditional Crafts, Siirt University, Siirt, Turkey
[2] Department of Mechanical Engineering, Hasan Kalyoncu University, Gaziantep, Turkey
[3] Department of Nanoscience and Nanotechnology, Erciyes University, Kayseri, Turkey

Received: 14 June 2024
Accepted: 15 July 2024
Published online: 26 July 2024

ABSTRACT

The polyacrylonitrile multifilament yarn underwent a multistep heat treatment process including stabilization times ranging from 5 to 75 min following impregnation with a 30% ethylenediamine (EDA) aqueous solution. A series of measurements were employed to determine the structure and properties of thermally stabilized PAN samples. These included fiber thickness, fiber density, flame testing, tensile testing, X-ray diffraction, thermal analysis (differential scanning calorimetry and thermogravimetric analysis), and infrared spectroscopy. The results from XRD and IR spectroscopy indicated that the rate of aromatization reactions increased with longer stabilization times. A detailed examination of the XRD curves obtained through curve-fitting procedures suggested a rapid transformation of the original structure into a disordered amorphous phase containing pre-graphitic domains, evidenced by a gradual reduction in the degree of apparent crystallinity of the original PAN sample. The integration of EDA before the thermal stabilization stage significantly reduced the cyclization time of nitrile groups in the PAN polymer structure, thereby accelerating the stabilization reactions. This chemical pretreatment also improved the thermal stability of the samples by promoting oxidative cross-linking of the PAN polymer chains. After a 75 min multistep stabilization, the carbon yield at 1000 °C was 70.5%. Conversion index values, calculated using IR, XRD, and DSC methods, were 98.3%, 94.8%, and 89.5% respectively for the 75 min sample. These findings highlight the importance of EDA in accelerating the formation of an aromatic structure, which is critical for withstanding the high temperatures of subsequent carbonization stages.

Handling Editor: Stephen Eichhorn.

Address correspondence to E-mail: kemalsahintuncel@gmail.com
E-mail Addresses: tuba.demirel@hku.edu.tr; ismailkaracanxxx@gmail.com

https://doi.org/10.1007/s10853-024-10033-8

GRAPHICAL ABSTRACT

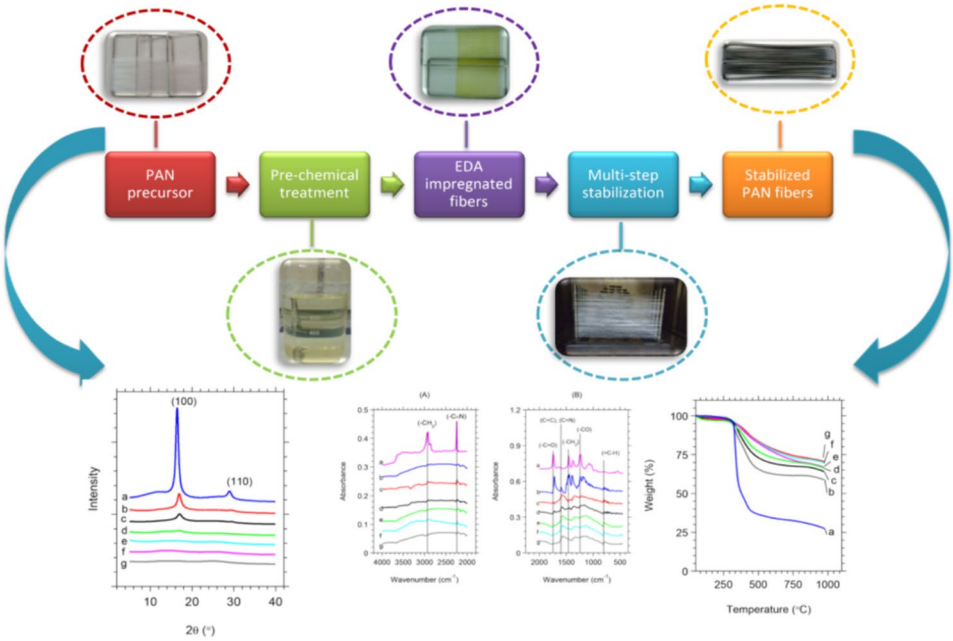

Introduction

The thermal oxidative stabilization (TOS) process is crucial in determining the ultimate tensile properties of carbon fibers. For this reason, ensuring comprehensive thermal stabilization of the PAN precursor is essential [1]. Thermal stabilization of the precursor multifilament bundle in an air atmosphere provides the fibers with the ability to withstand the elevated temperatures encountered in later stages, such as carbonization. Typically, the carbon fiber production process begins with the initial step of thermal stabilization in an air atmosphere, involving temperatures below 400 °C, followed by carbonization in a nitrogen environment spanning a temperature range of 800 to 1600 °C [2]. Carbon fibers are produced through a procedure that includes impregnation with flame-retardant chemical materials, thermal stabilization reactions in an air atmosphere, carbonization, and graphitization in an inert atmosphere (Fig. 1).

Although previous studies have explored alternative materials such as rayon [3], pitch [4], and lignin [5] as potential carbon fiber precursors, PAN fibers continue to be the preferred choice in today's market. The large-scale commercialization of PAN-based carbon fibers is challenging because of the high costs linked to the energy-intensive stabilization and carbonization processes [6]. The TOS stage uses the most energy during carbon fiber production [7]. So, the acceleration of this stage can help lower the cost of carbon fibers by reducing energy consumption. During the TOS stage, the C≡N groups in the linear PAN polymer transform into C=N groups (Fig. 2), creating a more stable structure with better thermal stability [8]. This ladder-like or aromatic polymer structure helps protect the samples from high temperatures and reduces mass loss [9]. However, the current long period of TOS for PAN precursors means there is a need to explore alternative physical and chemical methods for stabilization [10, 11]. Chemical methods involve treating PAN fibers with various chemicals before the TOS stage to speed up the stabilization process. Previous studies have used chemicals like ammonium dihydrogen phosphate [12], potassium permanganate [13], ferric chloride [14], boric acid [15], guanidine hydrochloride [16], guanidine carbonate [17], ammonium persulfate [18], ammonium bromide [19], mixture of ammonium bromide, phosphoric acid, and urea [20] and a combination of hydroxylamine hydrochloride with monoethanolamine [21] for this purpose.

In the present work, PAN fibers were chemically modified by treatment with EDA before thermal stabilization. The impact and effectiveness of EDA pretreatment on the thermal stabilization of PAN

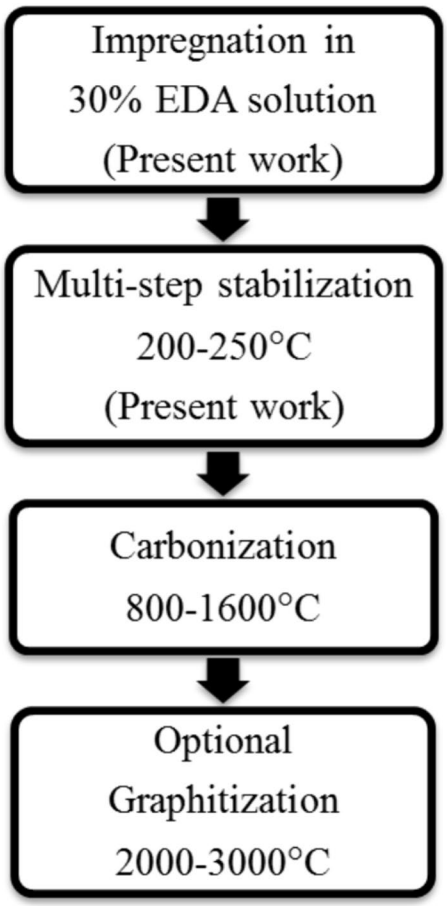

Figure 1 A schematic representation of the production process for PAN-based carbon fiber.

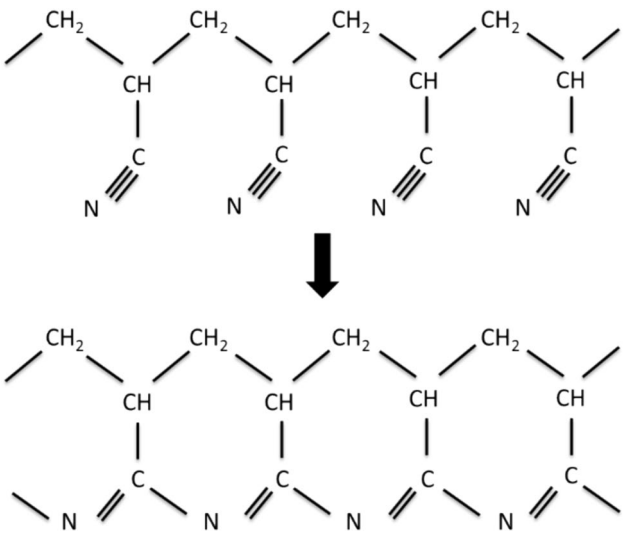

Figure 2 Conversion of linear PAN polymer chain to cyclized structure during TOS process [8].

multifilament yarn have not been widely studied before. So, a detailed experimental investigation was carried out to explore the potential use of EDA as an impregnation agent to improve the thermal stabilization reactions of PAN multifilament. The main goal of this work was to look at how the chemical impregnation method affects the structure and properties of PAN multifilament yarn using a multistep thermal stabilization approach, commonly used by carbon fiber manufacturers for the TOS process. Various techniques such as measuring fiber thickness, linear density, fiber density, tensile strength, XRD, thermal analysis (DSC, TGA), and FT-IR spectroscopy were used to evaluate the effectiveness of EDA impregnation on structural transformation.

Experimental

Materials and methods

The PAN multifilament bobbin was provided by AKSA Acrylic AS in Turkey and ethylenediamine ($NH_2CH_2CH_2NH_2$) was bought from Sigma-Aldrich. The PAN precursor was first cleaned in a solution of water and ethanol to remove surface dirt. Then, it was soaked in a 30% EDA solution at 90 °C for 60 min. The solution pH was 13.6 at room temperature. EDA binds to PAN nitrile groups via amine functional groups as shown in Fig. 3. EDA reduces the time needed for the cyclization of PAN polymer [22]. The pretreated PAN multifilament contained 26.7% EDA on a dry basis. The chemical loading percent was calculated considering the weight difference between the original (untreated) PAN and EDA-impregnated samples. The next step was a multistep thermal stabilization process, performed at temperatures between 200 and 250 °C for various times ranging from 5 to 75 min, as shown in Fig. 4. Careful control of the heating rate is crucial during the TOS stage to achieve the best results [23]. The test samples were securely wrapped around stainless steel rods without applying additional tension to maintain the molecular orientation during thermal stabilization. Apart from this process, no additional tension was applied to the fibers.

To evaluate the burning behavior, the experimental samples were directly exposed to an open flame. Their burning behaviors were categorized as either burning or flameproof. Color changes after the TOS procedure were noted through visual observation, without using

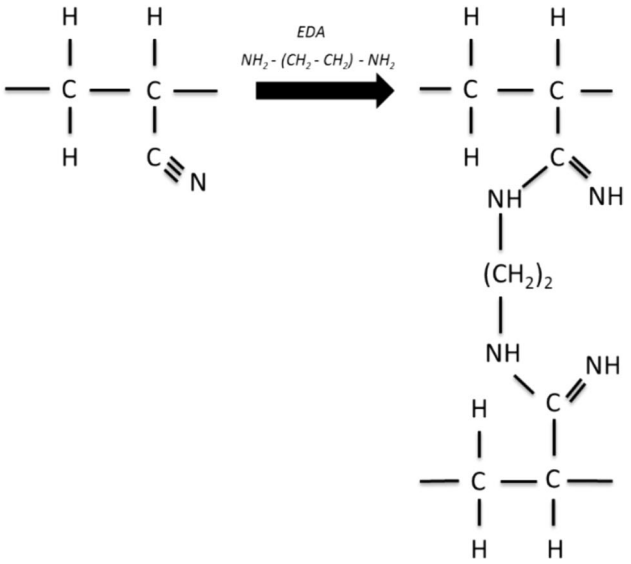

Figure 3 Interaction between linear PAN and EDA [24].

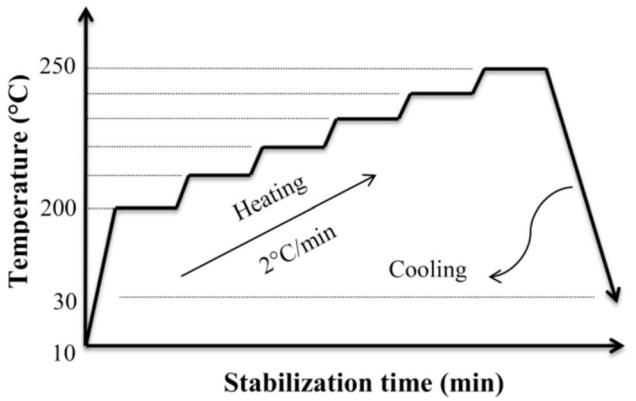

Figure 4 Multistep thermal stabilization procedure.

any special devices. The linear density of the PAN sample was obtained by evaluating the weight (g) per unit length (m). To measure the thickness of the fiber, 20 measurements were taken from each of 5 different filaments, and the result was calculated as the average. Fiber density values were obtained by constructing a density column using solutions of isopropyl alcohol (0.79 g cm^{-3}) and perchloroethylene (1.62 g cm^{-3}) at room temperature. The results were calculated as the average value of 5 different samples.

For TGA thermograms, the samples were heated at a rate of 10 °C min^{-1} until they reached a maximum temperature of 1000 °C using a Perkin Elmer TGA Diamond system. To ensure an inert atmosphere, a continuous flow of nitrogen gas was maintained at a rate of 200 ml min^{-1} throughout the experiments. The DSC experiments were conducted using the Perkin Elmer Diamond DSC system. Samples, weighing approximately 5 mg each, were analyzed. The heating rate for the DSC analysis was 10 °C min^{-1}, with a maximum temperature of 400 °C. FT-IR spectroscopy experiments were performed using the Perkin Elmer FT-IR Spectrum 400 spectrometer. The scan range was from 4000 to 500 cm^{-1}, with a wavenumber resolution of 2 cm^{-1}. X-ray diffraction measurements were carried out using a Bruker AXS D8 X-ray diffractometer, with the 2θ angle ranging from 5° to 40°. Mechanical properties were evaluated using a Prowhite tensile machine, with measurements performed at a constant drawing ratio of 5 mm min^{-1} and a gauge length of 20 mm. The reported results were averaged from 20 tensile tests.

Data analysis

The X-ray conversion index [25] was computed according to Eq. (1), where Io corresponds to the intensity at $2\theta = 16.4°$ for the original sample, and I corresponds to the intensity at $2\theta = 16.4°$ for the stabilized samples.

$$\text{X} - \text{ray Conversion index (\%)} = \frac{I_0 - I}{I_0} \times 100\% \quad (1)$$

X-ray crystallinity [26] was obtained from Eq. (2). Overall, the formula compares the intensity of the specific crystalline peak to the total intensity of the diffraction pattern to estimate the degree of crystallinity in the sample.

$$\chi_c = \frac{\text{Area under all the crystalline peaks}}{\text{Area under all crystalline and amorphous peaks}} \times 100\% \quad (2)$$

The d-spacing was calculated using Bragg's law Eq. (3), where λ is the wavelength of the X-ray beam; θ is the Bragg angle.

$$n.\lambda = 2d\,\text{Sin}(\theta) \quad (3)$$

The DSC-conversion index [27] was determined through the utilization of Eq. (4), where ΔH_o indicates the enthalpy of the original sample, ΔH indicates the enthalpy of the stabilized samples.

$$\text{DSC} - \text{Conversion index (\%)} = \frac{\Delta H_o - \Delta H}{\Delta H_o} \times 100\% \quad (4)$$

Table 1 Observation of changes in color and burning behavior of samples after the multistep thermal stabilization

Stabilization time (min)	Color (observationally)		Burning behavior (flame testing)	
	Reference sample	EDA impregnated	Reference sample	EDA impregnated
Original	White		Burns quickly	
5	Brown	Light Black	Burns quickly	Burns
15	Dark Brown	Light Black	Burns quickly	Burns slowly
30	Blackish	Blackish	Burns	Partially burns
45	Blackish	Black	Burns slowly	Partially flameproof
60	Black	Black	Partially burns	Fully flameproof
75	Black	Black	Partially burns	Fully flameproof

The IR-conversion index [28] was obtained from Eq. (5), where I_0 is the conjugated band intensity at ~ 1585 cm^{-1}, I_N is the nitrile band intensity at ~ 2242 cm^{-1}.

$$\text{IR} - \text{Conversion index (\%)} = \frac{I_0}{I_0 + I_N} \times 100\% \quad (5)$$

The limiting oxygen index (LOI) is a widely used parameter for characterizing the flammability of materials. It is the minimum oxygen concentration (%) required to support the combustion of polymeric materials. According to Eq. (6), The carbon yield (Cy) values at 1000 °C obtained from TGA were employed as the basis for calculating the LOI values [29].

$$\text{LOI} = 17.5 + 0.4\text{Cy} \quad (6)$$

Results and discussion

Physical properties

The TOS process encompasses several parameters, including stabilization temperature, heating rate, stabilization time, and tension, with temperature being the most critical factor. Incorrect process parameters can result in either insufficient or excessive fiber stabilization. Thermal stabilization involves an exothermic reaction, so a gradual heating approach is necessary to prevent sudden weight loss. In this experimental work, the temperature was gradually increased within the range of 200–250 °C.

Reference samples were beneficial in uncovering the accelerating effect of EDA impregnation on the thermal stabilization of PAN samples. These samples underwent multistep stabilization directly, without any chemical pretreatment. Thus, it was possible to compare the changes in physical properties of both the reference and EDA-impregnated samples after stabilization. Table 1 presents the observation of changes in color and burning behavior of the samples for each period of the multistep TOS process. Heat treatments caused color changes in the fibers, turning the original white hue of the original PAN fibers to black as stabilization time increased. This change signifies a structural transformation in PAN fibers, corroborated by earlier studies [17–19, 30]. The samples treated with 30% EDA and stabilized for 60 min passed the flame test, showing they could withstand the high temperatures of carbonization. In contrast, the reference sample, even after 75 min of stabilization, did not achieve sufficient thermal stability.

Table 2 presents changes in the physical properties of the samples for each period of the multistep TOS process. After 30% EDA impregnation, the PAN samples had a linear density of 75.6 tex and a fiber thickness of 23.3 μm. With increasing stabilization time, fiber thickness and linear density values decreased, while fiber density values increased. The EDA-treated and stabilized for 75 min sample showed a decrease in fiber thickness from 22 to 18.2 μm due to mass loss from structural changes. While the reference samples also had reduced fiber thickness over time, the decrease was more prominent in the EDA-treated samples [31]. After 75 min of multistep stabilization, there was a 17.3% reduction in fiber thickness compared to the precursor PAN multifilament bundle. This decrease in fiber thickness was also in line with the literature [32].

The fiber density value offers valuable insights into the changes in the structure of PAN fibers subsequent to the TOS process. It serves as a main parameter, particularly for assessing the effectiveness of the thermal stabilization process. Ideally, stabilized samples

Table 2 Changes in the physical properties of samples after the multistep thermal stabilization

Stabilization time (min)	Linear density (tex)		Fiber thickness (μm)		Fiber density (g cm^{-3})	
	Reference sample	EDA impregnated	Reference sample	EDA impregnated	Reference sample	EDA impregnated
Original	59.7		22		1.18	
5	59.6	60.1	21.8	22.1	1.19	1.25
15	58.6	59.3	21.2	21.7	1.21	1.29
30	58.5	58.5	20.9	20.6	1.26	1.33
45	58	57.4	20.2	19.3	1.31	1.38
60	57.8	56.8	19.9	18.9	1.33	1.41
75	57.6	56	19.2	18.2	1.35	1.42

Table 3 Changes in the mechanical properties of experimental samples after the multistep thermal stabilization

Stabilization time (min)	Tensile strength (MPa)		Extension at break (%)		Elastic modulus (GPa)	
	Reference sample	EDA impregnated	Reference sample	EDA impregnated	Reference sample	EDA impregnated
Original	262 ± 24		11.6 ± 1.8		13.9 ± 0.9	
5	200 ± 27	187 ± 20	9.2 ± 2.0	6.3 ± 1.0	11.1 ± 1.0	10.0 ± 0.7
15	175 ± 15	162 ± 19	6.5 ± 1.2	4.1 ± 1.0	11.5 ± 1.2	10.3 ± 0.6
30	170 ± 14	154 ± 17	4.1 ± 0.5	3.6 ± 0.9	12.3 ± 0.7	10.5 ± 0.6
45	158 ± 18	123 ± 13	3.4 ± 1.1	2.0 ± 0.4	12.1 ± 1.3	11.3 ± 1.6
60	160 ± 17	122 ± 17	2.9 ± 0.6	1.8 ± 0.4	12.2 ± 1.0	11.5 ± 0.8
75	159 ± 12	104 ± 16	2.7 ± 0.6	1.1 ± 0.4	13.0 ± 0.8	12.0 ± 1.4

should have fiber density values between 1.34 and 1.39 g cm^{-3} [33]. However, EDA-treated samples showed increased density values up to 1.42 g cm^{-3} in this work. In contrast, the density value of the reference sample stabilized for 75 min only reached 1.35 g cm^{-3}. These density increases suggest the start of cyclic structure formation [34]. Nunna et al. [35] reported an inverse relationship between fiber density values and the applied tension, indicating that higher tension hinders the formation of a cyclized structure. This could explain the higher density values observed in the stabilized PAN samples at 60 and 75 min, as no additional tension was applied to the fibers in the current work. Moreover, it has been proposed that achieving a density of 1.60 g cm^{-3} is necessary to obtain a fully aromatized structure [36].

Mechanical properties

The mechanical properties of both original PAN fiber and thermally stabilized samples are detailed in Table 3 and Fig. 5. The tensile strength values for the EDA-treated samples decrease from 262 to 104 MPa as the stabilization time increases. The same trend is observed for the elongation at break values, which decrease from 11.6 to 1.1% as the stabilization time lengthens. After 5 min of thermal stabilization for the EDA-treated sample, the tensile strength showed a reduction of roughly 28%, dropping to 187 MPa compared to the initial tensile strength of 262 MPa in the original PAN multifilament bundle. Then, the tensile strength continued to decline, reaching 104 MPa after 75 min of stabilization.

This corresponded to a gradual decrease of approximately 60% in tensile strength compared to the original fibers after a 75 min of thermal stabilization. Throughout the TOS reactions, the transformation from C≡N to C=N and C=C bonds takes place via intermolecular cross-linking reactions. This structural transformation results in a significant dissipation of cohesive energy within the polymer chains, leading to a gradual decline in mechanical properties [37]. The extent of tensile strength reduction can be inferred by evaluating the degree of conversion from C≡N to C=N. Similarly, the tensile strength values of the reference sample decreased over time, dropping to 159 MPa for

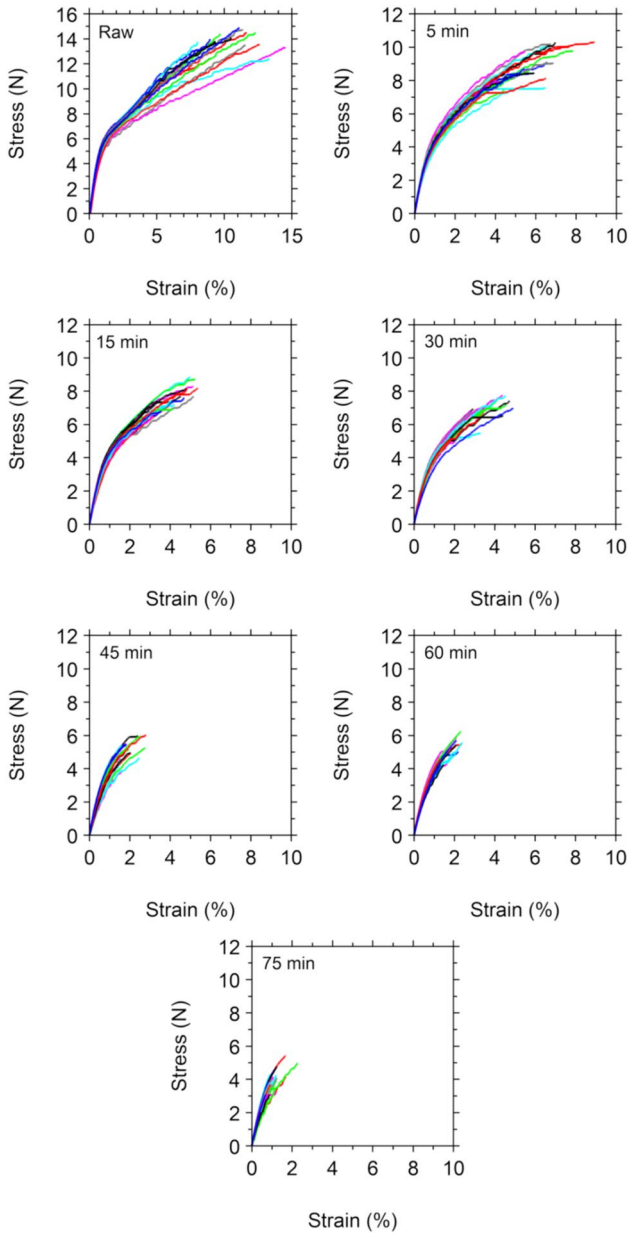

Figure 5 Stress–strain curves of EDA-impregnated and stabilized samples.

the sample stabilized for 75 min. This trend of mechanical properties decreasing during the TOS process is consistent with findings from other studies [31, 37–39]. When comparing the tensile strength values of the reference and EDA-treated samples, it's clear that while the reference samples have better mechanical properties, they still lack sufficient thermal stability. These samples require more time to achieve the desired

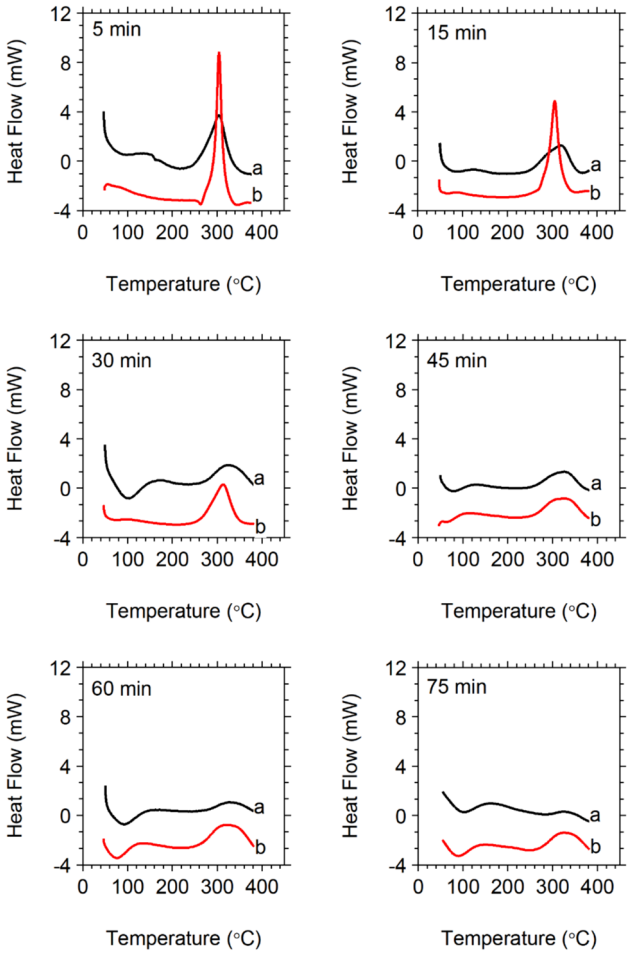

Figure 6 DSC thermograms **a** EDA-impregnated and stabilized **b** reference.

thermal stability. This shows that EDA-integration accelerates the thermal stabilization of PAN samples.

The elastic modulus of the EDA-treated sample decreased to 10 GPa after 5 min of stabilization, marking a 28% decrease. Then, it gradually rose to 12 GPa after 75 min of stabilization. The application of tension during the TOS process holds critical importance in shaping the mechanical properties by effectively enhancing the molecular alignment of the polymer chains. Increasing the tension applied to the fibers improves their mechanical properties. Additionally, various approaches have been proposed to enhance the mechanical properties of PAN-based carbon fibers [40, 41].

Thermal properties

The DSC thermograms play a vital role in the thermal analysis of experimental samples, providing valuable insights into molecular-level structural transformations. To demonstrate the effect of EDA impregnation on structural changes during thermal stabilization, reference samples directly stabilized without chemical pretreatment were utilized. DSC thermograms were generated for each thermal stabilization time (Fig. 6) to assess the difference in thermal properties between EDA-pretreated and reference samples. The decrease in the exothermic peak area, originating from the ladder-like polymer structure, results in the complete elimination of the exothermic peak as stabilization progresses, indicating the completion of cyclization reactions [42]. Barua and Saha [43] reported that cyclization reactions exhibit the highest activation energy among the reactions taking place during thermal stabilization. A chemical pretreatment of the PAN precursor is expected to accelerate the process by reducing the activation energy. Analysis of the data presented in Fig. 6 revealed a decrease in the exothermic peak area and an increase in peak width with prolonged stabilization. Moreover, the exothermic peak heights decreased in both the EDA-pretreated and reference samples throughout the stabilization lengthy. In the 5 min EDA-pretreated sample, there was a significant reduction in peak height from about 13 to 4.5 mW, while the reference sample showed a reduction in peak height to about 12.4 mW at the same stabilization time (Fig. 7b). These findings provide strong evidence of the time-saving impact of EDA impregnation on the TOS duration, leading to an expedited stabilization process. Figure 7a presents the conversion index values obtained from the data of DSC thermograms, using Eq. (4). As the stabilization time is extended, the DSC-conversion index value demonstrated a proportional increase. In particular, the sample subjected to 75 min of EDA pretreatment yielded a DSC-conversion index value of 89.5%, while the reference sample achieved a DSC-conversion index value of 70.6% at the same stabilization time.

Figure 8 illustrates the TGA thermograms for both the original and stabilized samples. The analysis of TGA findings aims to determine the carbon yield, a significant parameter for evaluating the thermal stabilization of PAN samples. During the carbonization process, weight loss is observed in the stabilized PAN fibers as various organic by-products are

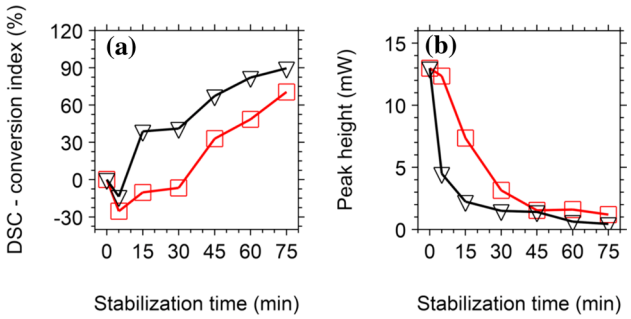

Figure 7 **a** DSC-conversion index and **b** exothermic peak height (□) reference (Δ) EDA-impregnated.

eliminated from the molecular structure. Notably, in the temperature range of 200 °C and 600 °C, there are different approaches to removing non-carbon elements from the precursor PAN. The dehydrogenation process primarily involves the liberation of hydrogen in the form of water vapor, while the elimination of other elements occurs in the form of nitrogen gas, hydrogen cyanide, carbon dioxide, carbon monoxide, water vapor, and oxygen gas.

The presence of ladder-like structures formed through cross-linking reactions led to a broader temperature range of weight loss in the stabilized samples, in contrast to the narrower temperature range observed in the original PAN. Table 4 presents the carbon yield values obtained from TGA at 500 °C and 1000 °C, respectively, along with the LOI values calculated using the carbon yield at 1000 °C. 5 min stabilization period resulted in a carbon yield value of 65.8% at 500 °C and 58.8% at 1000 °C, while a stabilization time of 75 min resulted in a carbon yield value of 83.6% at 500 °C and 70.5% at 1000 °C. Considering the carbon yield value of the PAN precursor, which is 26.4% at 1000 °C, it becomes apparent that the capacity for weight retention improves with extended periods of stabilization. The values of LOI obtained from carbon yield values at 1000 °C using Eq. (6) increased from 28.1 to 45.7, as illustrated in Table 4. The TGA analysis clearly demonstrated that thermally stabilized PAN fibers exhibit enhanced thermal stability due to the occurrence of cross-linking reactions. The findings from this analysis provided evidence that carbon yield values increase with longer stabilization times.

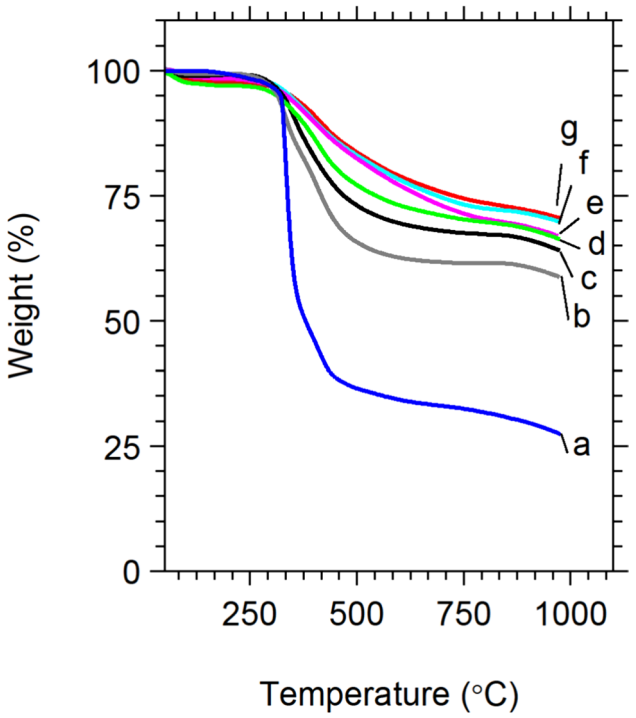

Figure 8 TGA thermograms **a** original PAN **b** 5 min **c** 15 min **d** 30 min **e** 45 min **f** 60 min **g** 75 min.

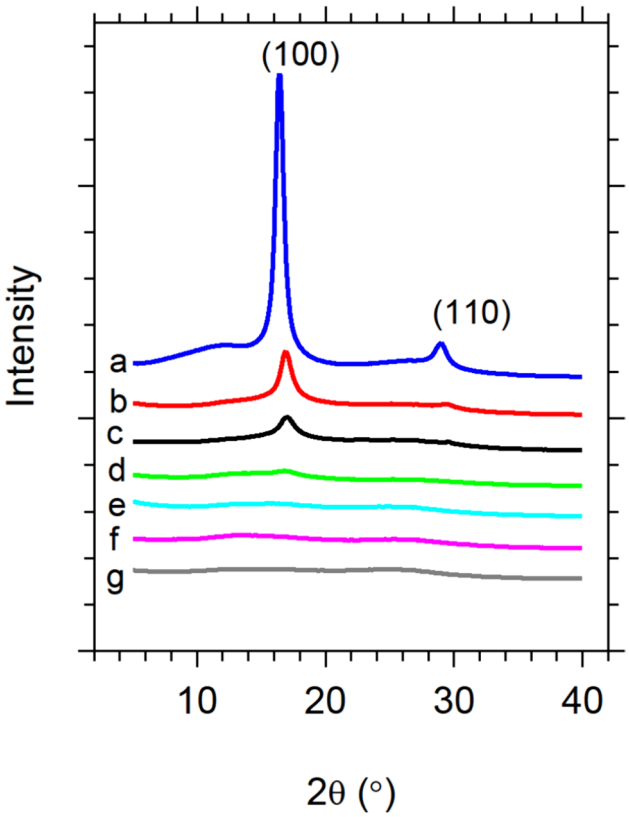

Figure 9 X-ray diffraction traces **a** original PAN **b** 5 min **c** 15 min **d** 30 min **e** 45 min **f** 60 min **g** 75 min.

Table 4 Carbon yield and calculated LOI values

Stabilization time (min)	Carbon yield at 500 °C (%)	Carbon yield at 1000 °C (%)	Calculated LOI (%)
Original	36.5	26.4	28.1
5 min	65.8	58.8	41
15 min	73.1	64.1	43.1
30 min	77.1	66.3	44
45 min	82.4	67	44.3
60 min	83	69	45.1
75 min	83.6	70.5	45.7

X-ray diffraction (XRD)

The change in the crystal structure of PAN after thermal stabilization was examined using the XRD technique, and traces obtained from XRD are displayed in Fig. 9. The original PAN had 2 angles of 16.43° for the (100) crystal planes and 30.31° for the (110) crystal planes. The XRD traces of the original PAN fiber show two peaks with d-spacings of 0.539 and 0.294 nm, indicating a hexagonal unit cell [44]. A curve-fitting technique was used to accurately determine the XRD peak parameters, and the curve-fitting of the XRD trace of the original PAN and EDA-impregnated and stabilized samples is shown in Fig. 10. An additional reflection was used to enhance the curve-fitted XRD traces during the curve-fitting stage. This reflection was attributed to a pre-graphitic (i.e., amorphous carbon) structure. It was observed that the laterally arranged structure underwent rapid disruption, which can be attributed to the advancement of stabilization reactions within the hexagonal crystal phase. As the stabilization time increased, the intensities of the (100) and (110) crystal planes persisted for periods ranging from 5 to 75 min. Additionally, the diffraction pattern showed a broad and less ordered peak (paracrystalline) with a d-spacing of 0.345 nm at approximately 25.5° 2θ, corresponding to the (002) reflection of the pre-graphitic structure, also known as the ladder/aromatic structure.

TOS reactions significantly impacted the crystal structure, affecting both the degree of crystallinity and the size of the crystallites in the laterally arranged structure. With increasing stabilization time, a gradual decline in the peak intensity of both (100) and (110)

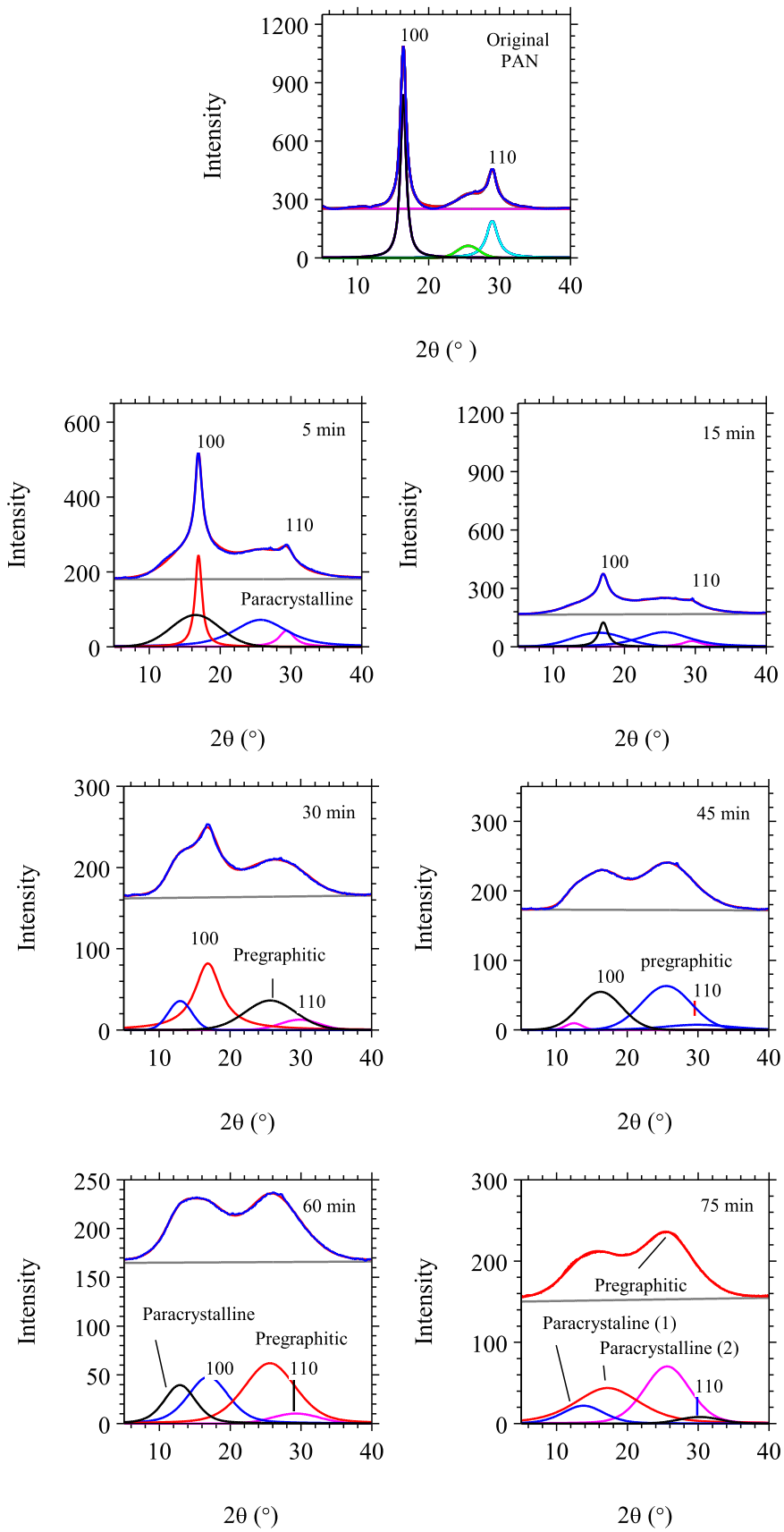

Figure 10 The curve-fitting of the XRD trace of original PAN and EDA-impregnated and stabilized samples.

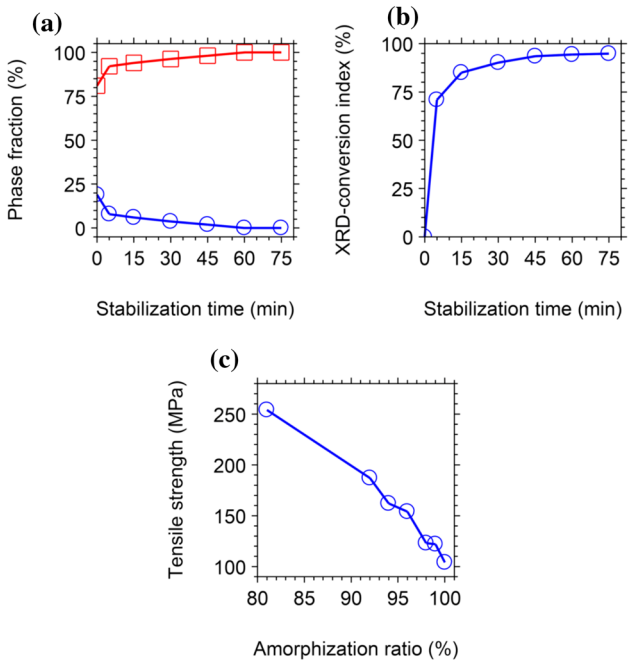

Figure 11 **a** Change of the % crystallinity (○) and % amorphous (□) fraction **b** XRD-conversion index **c** The correlation between the tensile strength and amorphization ratio.

crystal planes was observed. Similar behaviors have been documented in previous studies [17–19]. After a stabilization period of 5 min, there was about a 71% reduction in peak intensity at a 2θ angle of 16.43° and around 82% reduction in peak intensity at a 2θ angle of 30.31°. Using Eq. (2), it was noted that prolonged thermal stabilization led to an increase in amorphization (i.e., degree of disorder), ultimately resulting in a fully amorphous structure during the later stages of stabilization (Fig. 11a). The value of the conversion index obtained from the XRD data using Eq. (1) is shown in Fig. 11b. This index provided insight into the prediction of ladder-like structure formation during TOS reactions and exhibited an approximate 71% calculation after a 5 min stabilization period. Then, it gradually increased to about 95% after a final stabilization time of 75 min. It should also be noted that the data obtained from XRD only pertains to the crystalline regions. Figure 11c demonstrates a correlation between tensile strength values and the amorphization ratio. Specifically, as the amorphization ratio increased, the tensile strength values decreased.

Infrared (IR) spectroscopy

Using infrared spectroscopy is essential to understand how a multistep thermal stabilization process at different time intervals after EDA impregnation affects the initial functional groups in PAN. The IR spectra between 2000 and 500 cm^{-1} of the original PAN and stabilized samples are shown in Fig. 12b. Since the precursor PAN in this work contains at least 10% vinyl acetate monomeric units, the spectrum is expected to show specific infrared vibrations associated with these monomers. This situation led to the observation

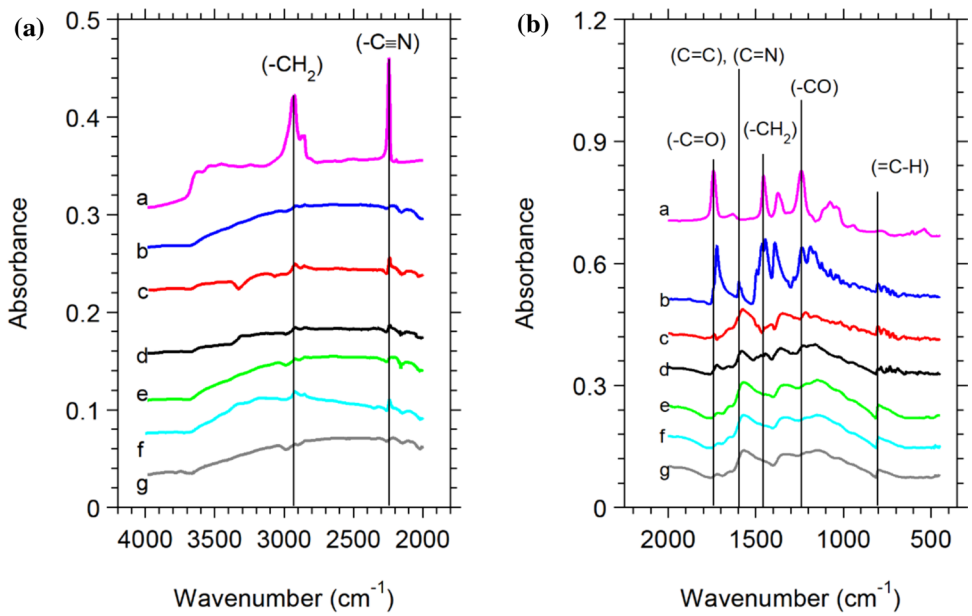

Figure 12 Infrared spectra between 4000 and 500 cm^{-1} wavenumbers **a** original PAN **b** 5 min **c** 15 min **d** 30 min **e** 45 min **f** 60 min **g** 75 min.

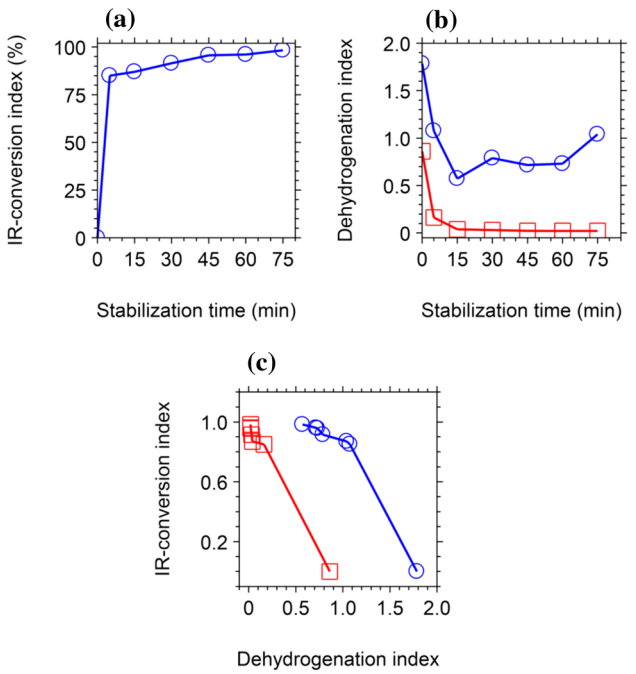

Figure 13 **a** IR-conversion index **b** dehydrogenation index and **c** The correlation between the IR-conversion index and dehydrogenation index (○) $A_{(1452)}/A_{(1368)}$, (□) $A_{(2920)}/A_{(1368)}$.

of some additional IR bands along with the IR band formed around 1736 cm^{-1} in the spectra [45].

The band at about 1736 cm^{-1}, assigned to the carbonyl (C=O) stretch, showed a significant reduction in intensity with increasing stabilization time and shifted toward a lower frequency (1730 cm^{-1}). This shift is interpreted as evidence of conjugation within the carbonyl band group [46]. Furthermore, a new set of conjugated bands, encompassing C=N groups, appeared within 1600–1550 cm^{-1} region of the IR spectra illustrated in Fig. 12. This signifies the transformation of nitrile (C≡N) groups into nitrilo (C=N) groups [47]. Stabilization in an oxygen environment is believed to facilitate dehydrogenation processes that convert C–C bonds into C=C bonds, forming aromatic structures [48]. Moreover, a newly identified conjugated band centered around 800 cm^{-1} is assigned to the C=C–H vibration. The IR spectra between 4000 and 2000 cm^{-1} of the original PAN and stabilized samples are shown in Fig. 12a. Even after just 5 min of stabilization, there was a substantial reduction in the intensity of the stretching band associated with methylene groups in the 3000–2900 cm^{-1} region. This decrease in methylene band intensity indicates the removal of hydrogen atoms from the structure due to dehydrogenation reactions. The reduced intensity of the nitrile band with prolonged stabilization suggests cyclization reactions are occurring.

Peak height values in terms of absorbance values were used to calculate dehydrogenation and IR-conversion index values. The TOS process occurs in the air medium because dehydrogenation reactions do not happen in an inert atmosphere. Oxygen contributes to the formation of functional groups essential for intermolecular cross-linking.

The data obtained using Eq. (5) showed that the original PAN structure quickly converts into an aromatized and cross-linked structure (Fig. 13a). The IR-conversion index rose to around 85% after 5 min of stabilization and peaked at about 98% after 75 min. Dehydrogenation index values, calculated by comparing absorbance ratios (A_{1452}/A_{1368} and A_{2920}/A_{1368}), clearly indicated hydrogen atom loss (Fig. 13b). Thus, it is supported that this index value is related to the removal of hydrogen atoms from the PAN structure. Infrared spectroscopy analysis confirmed that even with a brief 5 min stabilization process, the original PAN structure transforms into a cross-linked ladder structure. There's a direct correlation between the IR-conversion index and dehydrogenation index values. As dehydrogenation values decrease, IR-conversion index values increase (Fig. 13c).

Conclusions

This work positively demonstrated the effectiveness of EDA impregnation combined with a multistep thermal stabilization process for the PAN multifilament bundle, a vital precursor of carbon fiber production. Through comprehensive structural characterization, including density measurement, fiber thickness, tensile testing, XRD, TGA, DSC, and infrared spectroscopy, valuable insights were gained into the impact of EDA impregnation on the stabilization and transformation processes of PAN precursor. EDA pretreatment led to a notable increase in density from 1.18 to 1.38 g cm^{-3} within a relatively short stabilization period of 45 min. Achieving such a density value without chemical pretreatment would have required significantly longer times.

X-ray diffraction analysis showed the transition of thermally stabilized PAN samples toward an amorphous phase, marked by the gradual decrease in the intensity of the (100) crystal plane reflections

and the subsequent loss of crystallinity. This change was attributed to aromatization and dehydrogenation reactions, facilitated by oxidation reactions during stabilization. Infrared spectroscopy analysis provided evidence of accelerated aromatization and dehydrogenation reactions, supported by oxidation reactions, which led to a rapid reduction in the intensity of the nitrile and methylene bands as the stabilization time increased. A new band intensity observed around 1585 cm^{-1} was attributed to C=C and C=N groups, suggesting the conversion of nitrile groups to nitrile groups. Additionally, measurements conducted via reference samples using differential scanning calorimetry underscored the beneficial impact of EDA impregnation on molecular structural transformation during thermal stabilization. The faster decrease and eventual disappearance of the exothermic peak in EDA-pretreated samples indicated the cyclization of nitrile groups and the completion of cyclization reactions. Importantly, the multistep stabilization process coupled with EDA impregnation led to improved carbon yield values, reaching 83.6% and 70.5% at 500 °C and 1000 °C, respectively, compared to the original sample.

Conversion index values for the 75 min sample were 98.3%, 94.8%, and 89.5%, as calculated using IR, XRD, and DSC methods, respectively. These results show that the original PAN polymer structure significantly transformed into a thermally stable structure. This accelerated formation of the aromatic structure is crucial for enduring the high temperatures in the subsequent carbonization stage.

Acknowledgements

The assistance and cooperation of AKSA Acrylic AS (Turkey) are gratefully acknowledged for providing the PAN precursor filaments.

Author contributions

KŞT performed conceptualization, investigation, data acquisition, methodology, data analysis, writing—review, and editing. TD presented data analysis, data acquisition, writing—review, and editing. IK prepared writing—original draft, data analysis, review, and editing.

Funding

Open access funding provided by the Scientific and Technological Research Council of Türkiye (TÜBİTAK).

Data availability

The authors declare that the data supporting the findings of this work are available within the paper. Should any raw data files be needed in another format, they are available from the corresponding author upon reasonable request.

Declarations

Conflict of interest The authors declare no conflicts of interest with the research presented in this article. No ethical approval was necessary for this manuscript as it does not involve human or animal subjects. All authors have consented to the publication of this manuscript.

References

[1] Sedghi A, Farsani RE, Shokuhfar A (2008) The effect of commercial polyacrylonitrile fibers characterizations on the

produced carbon fibers properties. J Mater Process Technol 198:60–67. https://doi.org/10.1016/j.jmatprotec.2007.06.052

[2] Park S-J (2018) Carbon fibers, 2nd edn. Springer, Singapore

[3] Karacan I, Gül A (2014) Carbonization behavior of oxidized viscose rayon fibers in the presence of boric acid–phosphoric acid impregnation. J Mater Sci 49:7462–7475. https://doi.org/10.1007/s10853-014-8451-5

[4] Wazir AH, Kakakhel L (2009) Preparation and characterization of pitch-based carbon fibers. New Carbon Mater 24:83–88. https://doi.org/10.1016/S1872-5805(08)60039-6

[5] Chen J, Ghosh T, Tang T, Ayranci C (2022) Optimization of high-quality carbon fiber production from electrospun aligned lignin fibers. Polym Eng Sci 62:1256–1268. https://doi.org/10.1002/pen.25923

[6] Soulis S, Konstantopoulos G, Koumoulos EP, Charitidis CA (2020) Impact of alternative stabilization strategies for the production of PAN-based carbon fibers with high performance. Fibers 8:33–57. https://doi.org/10.3390/fib8060033

[7] Maghe M, Creighton C, Henderson LC, Huson MG, Nunna S, Atkiss S, Byrne N, Fox BL (2016) Using ionic liquids to reduce energy consumption for carbon fibre production. J Mater Chem A 4:16619–16626. https://doi.org/10.1039/C6TA06842A

[8] Shokuhfar A, Sedghi A, Eslami Farsani R (2006) Effect of thermal characteristics of commercialand special polyacrylonitrile fibres on the fabrication of carbon fibres. Mater Sci Technol 22:1235–1239. https://doi.org/10.1179/174328406X129887

[9] Yoo SH, Park S, Park Y, Lee D, Joh H-IK, Shin I, Lee S (2017) Facile method to fabricate carbon fibers from textile-grade polyacrylonitrile fibers based on electron-beam irradiation and its effect on the subsequent thermal stabilization process. Carbon 118:106–113. https://doi.org/10.1016/j.carbon.2017.03.039

[10] Golkarnarenji G, Naebe M, Badii K, Milani AS, Jazar RN, Khayyam H (2018) Production of low cost carbon-fiber through energy optimization of stabilization process. Materials 11:385–397. https://doi.org/10.3390/ma11030385

[11] Golkarnarenji G, Naebe M, Badii K, Milani AS, Jazar RN, Khayyam H (2018) Support vector regression modelling and optimization of energy consumption in carbon fiber production line. Comput Chem Eng 109:276–288. https://doi.org/10.1016/j.compchemeng.2017.11.020

[12] Sun J, Wu L, Wang Q (2005) Comparison about the structure and properties of PAN-based activated carbon hollow fibers pretreated with different compounds containing phosphorus. J Appl Polym Sci 96:294–300. https://doi.org/10.1002/app.21385

[13] Jie L, Wangxi Z (2005) Structural changes during the thermal stabilization of modified and original polyacrylonitrile precursors. J Appl Polym Sci 97:2047–2053. https://doi.org/10.1002/app.21916

[14] Karacan I, Erdogan G (2012) Ferric chloride assisted thermal stabilization of polyacrylonitrile precursor fibers prior to carbonization. J Inorg Organomet Polym Mater 22:1016–1027. https://doi.org/10.1007/s10904-012-9713-9

[15] Ouyang Q, Wang H, Cheng L, Sun Y (2007) Effect of boric acid on the stabilization of poly (acrylonitrile-co-itaconic acid). J Polym Res 14:497–503. https://doi.org/10.1007/s10965-007-9133-7

[16] Huang J, Ouyang Q, Li M, Heng F, Ma H, Chen Y (2019) Thermal behavior and thermal stabilization of guanidine hydrochloride-modified acrylic fiber for preparation of low-cost carbon fiber. J Therm Anal Calorim 136:2195–2203. https://doi.org/10.1007/s10973-018-7848-9

[17] Tunçel KŞ, Rahman MdM, Demirel T, Karacan I (2022) The impact of guanidine carbonate incorporation on the molecular structure of polyacrylonitrile precursor fiber stabilized by a multistep heat treatment strategy. Polym Eng Sci 62:1081–1095. https://doi.org/10.1002/pen.25908

[18] Rahman MdM, Demirel T, Tunçel KŞ, Karacan I (2021) The effect of the ammonium persulfate and a multi-step annealing approach during thermal stabilization of polyacrylonitrile multifilament prior to carbonization. J Mater Sci 56:14844–14865. https://doi.org/10.1007/s10853-021-06209-1

[19] Demirel T, Rahman MdM, Tunçel KŞ, Karacan I (2022) A study on structural characterization of thermally stabilized PAN precursor fibers impregnated with ammonium bromide before carbonization stage. Fibers Polym 23:3046–3057. https://doi.org/10.1007/s12221-022-4901-x

[20] Hariri H, Tunçel KŞ, Karacan I (2024) Multi-step heating strategy during thermal stabilization of polyacrylonitrile multi-filament bundle before carbonization. Polym Int. https://doi.org/10.1002/pi.6665

[21] Sun X, Song J, Zhang J, Liu J, Ke H, Wei Q, Cai Y (2020) Effects of chemical pre-treatment on structure and property of polyacrylonitrile based pre-oxidized fibers. J Eng Fibers Fabr. https://doi.org/10.1177/1558925019898946

[22] Karacan I, Erdogan G (2012) The effect of ethylenediamine pretreatment on the molecular structure of thermally stabilized polyacrylonitrile fibers before carbonization. Polym Eng Sci 52:467–480. https://doi.org/10.1002/pen.22104

[23] Hou Y, Sun T, Wang H, Wu D (2008) Effect of heating rate on the chemical reaction during stabilization of polyacrylonitrile fibers. Text Res J 78:806–811. https://doi.org/10.1177/0040517507090500

[24] Tahaei P, Abdouss M, Edrissi M, Shoushtari AM, Zargaran M (2008) Preparation of chelating fibrous polymer by different diamines and study on their physical and chemical properties. Mater Werkst 39:839–844. https://doi.org/10.1002/mawe.200800364

[25] Yu M-J, Bai Y-J, Wang C-G, Xu Y, Guo P-Z (2007) A new method for the evaluation of stabilization index of polyacrylonitrile fibers. Mater Lett 61:2292–2294. https://doi.org/10.1016/j.matlet.2006.08.071

[26] Wu S, Gao A, Wang Y, Xu L (2018) Modification of polyacrylonitrile stabilized fibers via post-thermal treatment in nitrogen prior to carbonization and its effect on the structure of carbon fibers. J Mater Sci 53:8627–8638. https://doi.org/10.1007/s10853-017-1894-8

[27] Tsai J-S, Hsu H-N (1992) Determination of the aromatization index for oxidized polyacrylonitrile fibre by the differential scanning calorimetry method. J Mater Sci Lett 11:1403–1405. https://doi.org/10.1007/BF00729641

[28] Zhu Y, Wilding MA, Mukhopadhyay SK (1996) Estimation, using infrared spectroscopy, of the cyclization of poly(acrylonitrile) during the stabilization stage of carbon fibre production. J Mater Sci 31:3831–3837. https://doi.org/10.1007/BF00352799

[29] Van Krevelen DW, Hoftyzer PJ (1976) Properties of polymers, 2nd edn. Elsevier, New York

[30] Zhang X, Kitao T, Piga D, Hongu R, Bracco S, Comotti A, Sozzani P, Uemura T (2020) Carbonization of single polyacrylonitrile chains in coordination nanospaces. Chem Sci 11:10844–10849. https://doi.org/10.1039/D0SC02048F

[31] Hameed N, Sharp J, Nunna S, Creighton C, Magniez K, Jyotishkumar P, Salim NV, Fox B (2016) Structural transformation of polyacrylonitrile fibers during stabilization and low temperature carbonization. Polym Degrad Stab 128:39–45. https://doi.org/10.1016/j.polymdegradstab.2016.02.029

[32] Akia M, Cremar L, Seas M, Villarreal J, Valdez A, Alcoutlabi M, Lozano K (2018) High-throughput production with improved functionality and graphitization of carbon fine fibers developed from sodium chloride-polyacrylonitrile precursors. Polym Eng Sci 58:2047–2054. https://doi.org/10.1002/pen.24816

[33] Takaku A, Hashimoto T, Miyoshi T (1985) Tensile properties of carbon fibers from acrylic fibers stabilized under isothermal conditions. J Appl Polym Sci 30:1565–1571. https://doi.org/10.1002/app.1985.070300421

[34] Arbab S, Zeinolebadi A (2013) A procedure for precise determination of thermal stabilization reactions in carbon fiber precursors. Polym Degrad Stab 98:2537–2545. https://doi.org/10.1016/j.polymdegradstab.2013.09.014

[35] Nunna S, Naebe M, Hameed N, Creighton C, Naghashian S, Jennings MJ, Atkiss S, Setty M, Fox BL (2016) Investigation of progress of reactions and evolution of radial heterogeneity in the initial stage of thermal stabilization of PAN precursor fibres. Polym Degrad Stab 125:105–114. https://doi.org/10.1016/j.polymdegradstab.2016.01.008

[36] Endrey AL (1982) The base-catalyzed transformation of polyacrylonitrile. J Polym Sci, Polym Chem Ed 20:2105–2116. https://doi.org/10.1002/pol.1982.170200814

[37] Ge Y, Fu Z, Deng Y, Zhang M, Zhang H (2019) The effects of chemical reaction on the microstructure and mechanical properties of polyacrylonitrile (PAN) precursor fibers. J Mater Sci 54:12592–12604. https://doi.org/10.1007/s10853-019-03781-5

[38] Liu Y, Liu Y, Shang L, Ao Y (2022) Study on the structural evolution of polyacrylonitrile fibers in stepwise heat treatment process and its relationship with properties. J Appl Polym Sci 139:52077–52094. https://doi.org/10.1002/app.52077

[39] Elagib THH, Hassan EAM, Fan C, Han K, Yu M (2019) Microwave pre-oxidation for polyacrylonitrile precursor coated with nano-carbon black. Polym Eng Sci 59:457–464. https://doi.org/10.1002/pen.24943

[40] Qin X, Lu Y, Xiao H, Zhao W (2013) Effect of heating and stretching polyacrylonitrile precursor fibers in steam on the properties of stabilized fibers and carbon fibers. Polym Eng Sci 53:827–832. https://doi.org/10.1002/pen.23328

[41] Raghavan V, Gulgunje PV, Gupta KK, Kamath MG, Liu Y, Pramanik C, Newcomb BA, Chae HG, Kumar S (2019) Correlation between inhomogeneity in polyacrylonitrile spinning dopes and carbon fiber tensile strength. Polym Eng Sci 59:478–482. https://doi.org/10.1002/pen.24947

[42] Jain MK, Balasubramanian M, Desai P, Abhiraman AS (1987) Conversion of acrylonitrile-based precursors to carbon fibres. J Mater Sci 22:301–312. https://doi.org/10.1007/BF01160585

[43] Barua B, Saha MC (2018) Studies of reaction mechanisms during stabilization of electrospun polyacrylonitrile carbon nanofibers. Polym Eng Sci 58:1315–1321. https://doi.org/10.1002/pen.24708

[44] Hu X, Johnson DJ, Tomka JG (1995) Molecular modelling of the structure of polyacrylonitrile fibres. J Text Inst 86:322–331. https://doi.org/10.1080/00405009508631337

[45] Karacan I, Erdogan G (2012) The influence of thermal stabilization stage on the molecular structure of polyacrylonitrile fibers prior to the carbonization stage. Fibers Polym 13:295–302. https://doi.org/10.1007/s12221-012-0295-5

[46] Grassie N, McGuchan R (1972) Pyrolysis of polyacrylonitrile and related polymers—VI. Acrylonitrile copolymers containing carboxylic acid and amide structures. Eur

Polym J 8:257–269. https://doi.org/10.1016/0014-3057(72)90032-8

[47] Clarke AJ, Bailey JE (1973) Oxidation of acrylic fibres for carbon fibre formation. Nature 243:146–150. https://doi.org/10.1038/243146a0

[48] Ouyang Q, Cheng L, Wang H, Li K (2008) Mechanism and kinetics of the stabilization reactions of itaconic acid-modified polyacrylonitrile. Polym Degrad Stab 93:1415–1421. https://doi.org/10.1016/j.polymdegradstab.2008.05.021